Energy dissipation rates, eddy diffusivity, and the Prandtl number: An in situ experimental approach and its consequences on radar estimate of turbulent parameters

François Bertin, Jean Barat, Richard Wilson

Radio Science, Volume 32, Number 2, Pages 791–804, March–April 1997

Energy dissipation rates, eddy diffusivity, and the Prandtl number: An in situ experimental approach and its consequences on radar estimate of turbulent parameters

Francois Bertin
Centre d'Etude des Environnements Terrestres et Planétaires, Saint Maur-des-Fossés, France

Jean Barat and Richard Wilson
Service d'Aéronomie du CNRS, Verrières le Buisson, France

Abstract. Different methods have been proposed to derive the energy dissipation rate and eddy diffusion coefficients from ST radar measurements. However, their validity is still questionable because they implicitly assume that the Prandtl number is always equal to one, an assumption which is not verified. An experimental approach to this question, using balloon-borne experiment results, is proposed in this paper in order to test the validity/invalidity of the methods generally used. In situ observations show that the potential temperature gradient is more efficiently (and probably more rapidly) eroded by the turbulent activity than the wind shear. As a consequence of this observational evidence already mentioned by *Browning and Watkins* [1970], the structure function constant for temperature fluctuations (C_T^2) is vanishing within fully developed turbulent layers and exibits maxima on their boundaries, while the structure parameter for wind fluctuations (C_V^2) presents a broad maximum within the same layer and is decreasing at its boundaries. Consequently, the gradient Richardson number R_i strongly varies within fully developed turbulent layers, from R_i close to zero (near their center) up to $R_i > 1$ (at their boundaries). By contrast, the flux Richardson number R_f, which describes the evolution of the ratio between buoyancy flux and turbulent energy production, remains apparently quasi-constant and close to its critical value during the erosion processes, so that the Prandtl number is not a constant close to unity but might also strongly vary during the turbulent life cycle. These results are in good agreement with laboratory experiments in statistically stable fluids reviewed by *Thorpe* [1973] and with experimental results obtained in the boundary layer [*Businger et al.*, 1971; *Gossard and Frisch*, 1987]. ST radar are generally not able to observe regions where the potential temperature gradient is eroded by the turbulent activity but may obtain strong responses on the boundaries of fully developed turbulent layers. This behavior does not affect the radar capability of estimating eddy dissipation rate ε and eddy diffusivity K_θ (or K_M) when complementary information on temperature profiles and humidity are available. It is shown that the "nonlocal" mean potential temperature gradient, the wind shear, and the flux Richardson number are the pertinent parameters allowing a correct estimate of the eddy dissipation rates and eddy diffusion coefficients, from C_n^2 (C_T^2) and rms turbulent vertical wind, in regions where the turbulent activity is observable by ST radars.

Paper number 96RS03691.
0048-6604/97/96RS-03691$11.00

1. Introduction

One of the primary goals of atmospheric microstructure measurements in the upper troposphere and lower stratosphere has been to estimate the vertical fluxes of mass, heat, momentum, etc, due to three-dimensional turbulence processes. Both in situ and remote techniques are employed. In situ techniques have successfully been used by many groups [e.g.,*Vinnichenko et al.*, 1973; *Lilly et al.*, 1974; *Thrane and Grandal,* 1981; *Thrane et al.*, 1987; *Barat and Bertin*, 1984b; *Lübken et al.*, 1987; *Lübken,* 1992; *Dalaudier et al.*, 1994]. However, all of these results applied only to a small amount of data. The increasing number of clear-air radars will allow radar methods, if proven reliable, to be applied in many more situations. The remote techniques using these radars are reviewed by *Hocking* [1985] and described in more details by, for example, *Ottersten* [1969], *Frisch and Clifford* [1974], *VanZandt et al.* [1978], *Crane* [1980], *Gage et al.* [1980], *Weinstock* [1981], *Woodman and Rastogi* [1984], *Sengupta et al.* [1987], and *Gossard and Sengupta* [1988].

Three independent methods for estimating the turbulent dissipation rate ε from the ST radar measurements are generally proposed. The first method uses the backscattered power and relies on the effect of eddy motions on the atmospheric refractive index. It requires additional measurements of temperature and humidity. Two other methods make use of the Doppler spectrum broadening by turbulent motions. Comparison

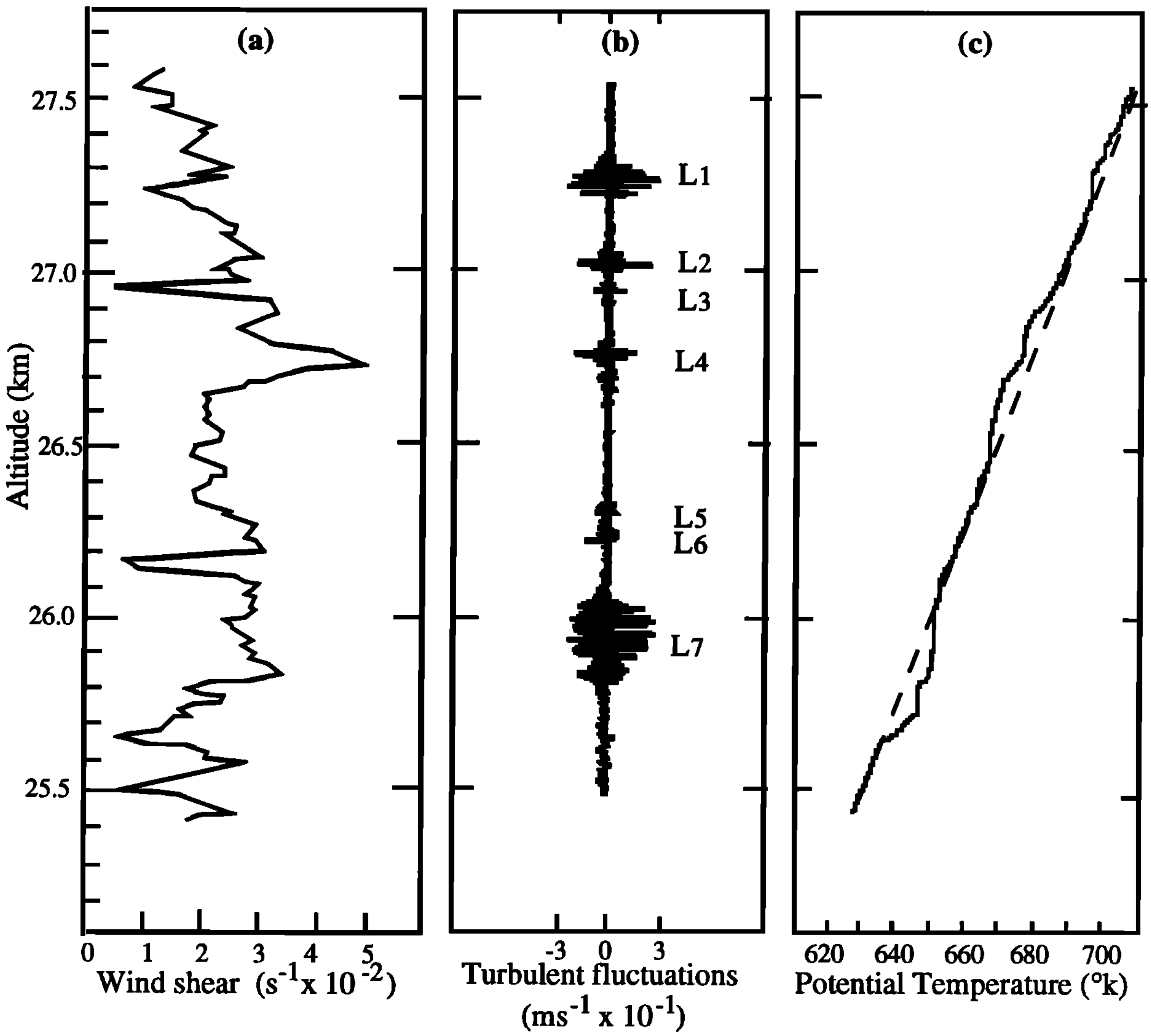

Figure 1. Vertical profiles of (a) wind shear, (b) turbulent wind fluctuations and (c) potential temperature obtained with balloon-borne high-precision anemometers and microhead thermistors, performed on April 28, 1978.

of results obtained by both power and width methods using a common data set has been done by *Cohn* [1995] using the Millstone Hill UHF radar and by *Delage et al.* [this issue] using the high-resolution UHF PROUST radar. However, as will be shown in more detail in the next section, some assumptions on the flux Richardson number, or the Prandtl number, are made in these procedures and introduce significant uncertainties in the final results because these parameters are up to now poorly known and may vary with time within turbulent layers, as stressed by *McIntyre* [1989], or *Moum* [1990].

In order to assess these procedures, we present in the following an analysis of some turbulence characteristics derived from in situ measurements performed on April 28, 1978, between 25.5 and 27.5 km by high-resolution balloon-borne instruments within seven turbulent layers with thicknesses varying between 10 and 250 m. The experimental description and the main results of this balloon experiment were published 12 years ago [*Barat and Bertin*, 1984b]. However, the results concerning the turbulent dissipation rate and the eddy diffusivity estimates have not yet been published and are analyzed in the present paper.

2. Instrumental Procedure and Basic Results

The experiment has been completely described previously [*Barat*, 1982; *Barat and Bertin*, 1984a; *Barat and Bertin*, 1984b]. Two gondola are hung below a zero-pressure balloon, 30 m diameter, at distance h1=100 m and h2=150 m. Each gondola is equipped with a highly sensitive ionic anemometer and a microhead thermister. Temperature and wind resolution are 0.015 K and 0.25 cm/s, respectively. A 16-Hz sampling rate and 12-bit words have been used for the numeric telemetry. During a slow descent of the ballon (0.3 m/s<V_Z<0.5 m/s), the gondola crossed seven turbulent regions (labeled L1 to L7) whose thickness varies from a few meters (L5) to 250 m (L7). Figure 1 shows the profiles of wind shear, turbulent wind fluctuations, and potential temperature in the region where the seven turbulent layers are observed. The mean wind shear is of the order of 2-5x10^{-2} s^{-1}, and the mean potential temperature gradient in nonturbulent regions is about 4x10^{-2} K m^{-1}. In the following, the results obtained within the seven layers are used, but the fully developed layer L7 is especially studied because it is interesting to better understand why only the boundaries of these layers are generally observed by ST radars.

Structure function analysis of wind and temperature turbulent fluctuations are performed at every 10-m-altitude interval. Elimination of possible contamination of the structure function by wind shear has been done by the method descibed by *Barat and Bertin* [1984a]. As the balloon is slowly descending, about 20-30 s are necessary for crossing the 10-m-altitude interval, so that 300-400 temperature and wind measurements are used for each structure function. During this time interval, the corresponding horizontal distance described by the balloon is about 80-90 m, so that the parameters derived from these structure functions are quite representative of the horizontal characteristics of the turbulent field. Profiles of structure parameters C_V^2 and C_T^2, energy dissipation rate ε , rms turbulent wind u_o , outer scale of turbulence Lo are systematically derived from these structure functions, while mean wind shear and potential temperature profiles are obtained by filtering the temporal series of wind shear and temperature measurements. From these values it is possible to derive the mixing lengh L_S, the buoyancy lengh L_B , the Richardson number, and the Prandtl number and also to estimate the eddy diffusivity for heat and momentum by the different approachs used in the literature.

2.1. C_T^2 and C_V^2 Profiles of Behavior Within a Turbulent Layer and Consequences on its Radar Detection

Several stages of turbulent configurations are observed. In layer L5 (Figure 1), whose thickness is about 10 m, the turbulence is apparently just beginning and the potential temperature gradient not yet eroded, while in layer L7, the potential temperature has been already quasi-mixed by the turbulent activity, making appear a weak potential temperature gradient (Figure 2a) bordered by a steeper gradient at its lower edge. As the wind shear is quasi-constant in layer L7 (Figure 1a), the local Richardson number profile (Figure 2a) closely follows the evolution of the temperature gradient. Its value is much smaller than the critical value (Ri_C=0.25) in the central part of the layer, while it is greater than one in its lower edge.

The structure parameter C_T^2 profile (Figure 2b) exhibits the same behavior: small values in regions of low temperature gradient and maxima near the boundaries. The corresponding values of the structure parameter C_n^2 for atmospheric refractive index (Figure 2b) are also vanishing within the layer and exhibit in the lower boundary a maximum slightly greater than 10^{-18} $m^{-2/3}$. As the C_n^2 minimum required for radar

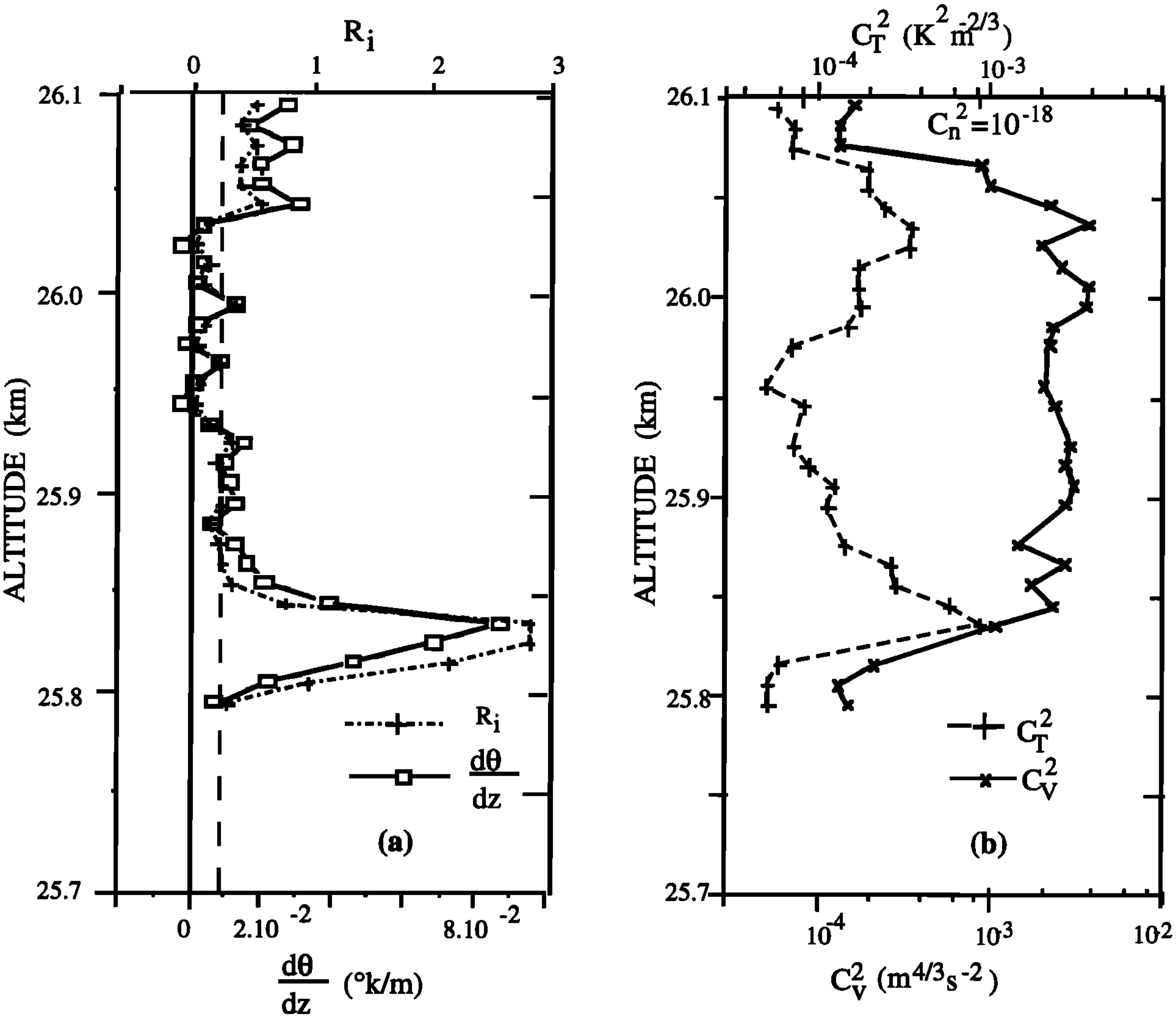

Figure 2. (a) Potential temperature gradient and local Richardson number profiles in layer L7 and (b) C_T^2 and C_V^2 profiles in the same region.

detection is of the order 3-6x10^{-19} $m^{-2/3}$, Figure 2b shows that the boundaries of well-developed turbulent layers are the only regions which are observable by ST radars. This characteristic behavior has already been noticed by *Browning and Watkins* [1970] in the boundary layer by using a Frequency Modulated Continuous Wave high-resolution radar. On the other hand, the structure parameter C_V^2 (Figure 2b) shows a quite different shape, as already mentioned by *Barat and Bertin* [1984b], with a broad maximum within the turbulent layer and a sharp decrease at the boundaries. These results strongly suggest that the turbulent erosion is much more efficient for temperature gradients than for wind shears, so that vanishing temperature fluctuations and C_T^2 within a turbulent layer do not signify (as shown by equation (1)) a lack of turbulent activity but only an impossibility to detect it from temperature measurements in the case where the potential temperature gradient tends toward zero.

$$C_T^2 = -2.8\,\overline{w'\theta'}\,\frac{d\theta}{dz}\,\varepsilon^{-1/3} \qquad (1)$$

An important consequence of this correlation between C_T^2 and $d\theta/dz$ evolution concerns their ratio $C_T^2/(d\theta/dz)$, which is very badly defined in regions where the potential temperature gradient is eroded by turbulence, so that any estimate of turbulent parameters requiring the knowledge of this ratio will furnish poor or spurious results in these regions. However, as mentioned above, this situation cannot be observed by ST radars, only the in situ measurements analysis encounters this difficulty.

Figure 2 also shows that the gradient Richardson number

$$R_i = \frac{g}{\theta}\frac{d\theta/dz}{(du/dz)^2} \tag{2}$$

is greater than one in the lower edge of layer L7, while the turbulent activity remains important (both for C_T^2 and C_V^2). This is somewhat contradictory to the theory which predicts that turbulence cannot continue in stratified regions where R_i becomes greater than one. This apparent contradiction suggests the gradient Richardson number might not be the pertinent parameter for monitoring the evolution of dynamical instabilities within a fully developed turbulent layer. This point is analyzed in the next section.

2.2. Flux Richardson Number, Gradient Richardson Number, and Prandtl Number

In this section we show that the flux Richardson number R_f instead of Ri is the pertinent parameter for monitoring the turbulence activity within turbulent layers. The flux Richardson number is defined as

$$R_f = \frac{B}{P} \tag{3}$$

where B is the buoyancy flux and P is the turbulent energy production.

$$B = -\frac{g}{\theta}\overline{w'\theta'} = K_\theta \frac{g}{\theta}\frac{\partial\theta}{\partial z} \tag{4}$$

$$P = -\overline{u'w'}\frac{du}{dz} = K_M\left(\frac{\partial u}{\partial z}\right)^2 \tag{5}$$

In these expressions, $\overline{w'\theta'}$, K_θ and $\overline{u'w'}$, K_M are the fluxes and eddy diffusivities for heat and momentum respectively.

When taking into account (2), (4), and (5), the flux and gradient Richardson numbers are tied by the relationship

$$R_f = \frac{K_\theta}{K_M}R_i = \frac{1}{P_r}R_i \tag{6}$$

where Pr is the Prandtl number.

For stationary turbulence, and if the third-order parameters (divergence terms) are neglected, the energy dissipation rate ε can be written [*Tatarskii*, 1961]

$$\varepsilon = P - B \tag{7}$$

Experimentally, the energy dissipation rate may be directly estimated from the structure functions of wind fluctuations (giving C_V^2) and by the relationship

$$C_V^2 = 2\,\varepsilon^{2/3}. \tag{8}$$

The flux Richardson number can be experimentally obtained by two different methods. The first one consists in estimating B and P from C_V^2, C_T^2, and $d\theta/dz$. The second one is based on mixing length and buoyancy length estimates.

In the first method, the heat flux $\overline{w'\theta'}$ and B are given by (1) and (8) (however, as stressed in the previous section, B is badly estimated in regions of weak potential temperature gradient). The turbulent energy production P is then obtained from (7), and finally R_f is given by (3). Figure 3a gives the profile of R_f in L7 compared with the R_i profile, while the Prandtl number profile is given in Figure 3b. For the R_f and R_i determination, the mean wind shear and potential temperature gradient are determined from filtered temporal series of wind and temperature. In regions where both C_T^2 and potential temperature gradient are not vanishing (e.g., in the lower boundary of L7), the flux Richardson number is generally found to be in the range 0.15-0.25, while R_i is strongly varying. As a consequence, the Prandtl number is found to be highly variable, with values ranging from 0.1 to 20 within the layer. These results are in good agreement with R_f and Prandtl number values obtained in the boundary layer by *Kondo et al.* [1978] and *Gossard and Frisch* [1987]. In Figure 4 the P_r^{-1} evolution as a function of R_i obtained in layer L7 is given. For comparison, the curve-fits proposed by *Kondo et al.* [1978] and by *Gossard and Frisch* [1987] are shown. The observed fairly good agreement between results obtained in the boundary layer, as well as in a specific stratospheric turbulent layer, clearly indicates the P_r^{-1} versus Ri dependence is characterized by a well-defined shape, set up by a quasi-constant R_f value.

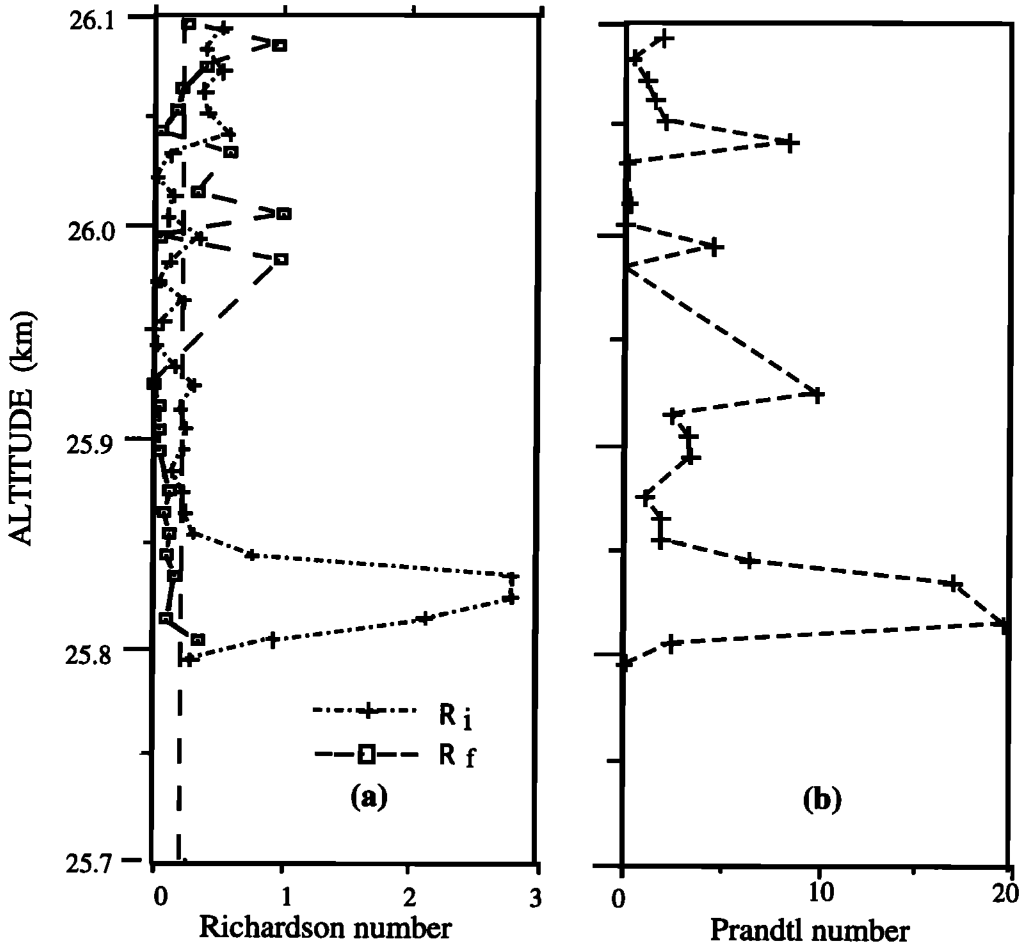

Figure 3. (a) Gradient and flux Richardson number profiles within turbulent layer L7 . The vertical dashed line corresponds to $R_i = R_f = 0.25$. (b) Prandtl number profile in the same layer.

The second method used to derive the flux Richardson number from the experimental data is based on the estimate of the mixing length. For an isotropic and homogeneous turbulence (assumption probably not fully justified for at least one of the seven turbulent layers taken into account in this study), the mixing length L_S , associated with the wind shear S , can be expressed, after *Tatarskii* [1961], and *Dillon* [1982] as

$$L_S = \frac{u_o}{S} = \frac{(\overline{u'w'})^{1/2}}{S} = \frac{R_i^{3/4}}{(1-R_f)^{1/2}} \frac{\varepsilon^{1/2}}{N^{3/2}} \qquad (9)$$

In this equation, u_o is the rms turbulent wind and $(\overline{u'w'})$ is the momentum flux.

The ratio u_o/S is systematically calculated from the structure functions (whose breakpoint is giving u_o) and the wind shear profile, so providing an estimate of the mixing length L_S. In the right-hand part of (9), the ratio $\varepsilon^{1/2}/N^{3/2}$ is often considered [*Dougherty*, 1961] as a rough estimate of the buoyancy length L_B. This expression of L_B may also be experimentally estimated from C_V^2 (provided by structure functions of wind fluctuations) and N (estimated from the filtered potential temperature profile). From (9) the theoretical expression of the ratio L_B/L_S is

$$\frac{L_B}{L_S} = \frac{\left(1-R_f\right)^{1/2}}{R_i^{3/4}} \qquad (10)$$

As shown by this equation, the ratio L_B/L_S is equal to zero when $R_f = 1$.

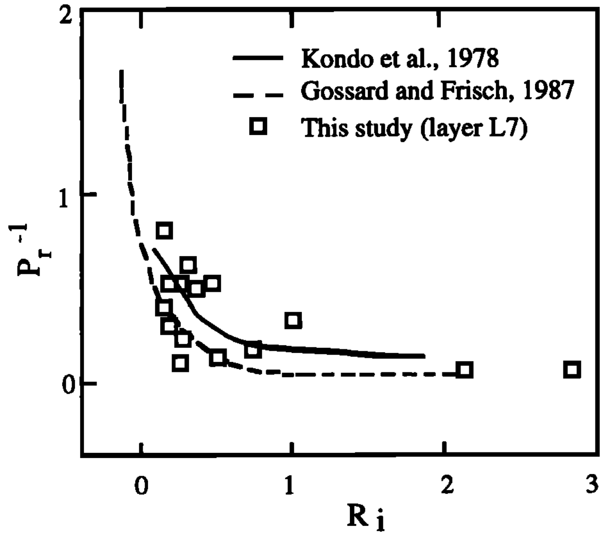

Figure 4. Results of measurements of Pr^{-1} versus Ri. Squares are data obtained from layer L7. For comparison, the solid curve is the "best fit" proposed by *Kondo et al.* [1978], while the dashed curve is the "best fit" proposed by *Gossard and Frisch* [1987]. Measurements performed with the balloon experiment in the stratosphere are found to be in good agreement with both previous studies realized in the boundary layer.

2.3. Experimental Results

As indicated above, the ratio L_B/L_S has been experimentally determined within the seven turbulent layers observed during the balloon descent. Figure 5 gives the experimental variation of this ratio as a function of the gradient Richardson number (also experimentally determined). The L_B/L_S variation exhibits a tendency to follow the empirical law

$$\frac{L_B}{L_S} = \frac{0.85}{R_i^{3/4}} \tag{11}$$

The only way to reconcile (10) and (11) is to assume that R_f remains approximatly constant, with a statistical mean value close to its initial critical value R_f =0.25 during the lifetime of the turbulence, whatever the observed evolution of the gradient Richardson number. These results are in good agreement with the laboratory experiments reviewed by *Thorpe* [1973].

One can see that both methods used to derive the flux Richardson number give similar results: R_f remains quasi-constant, with values in the range 0.15-0.30 during the turbulent activity, while the gradient Richardson number may strongly vary due to the erosion of the potential temperature gradient within well-developed turbulent layers and the appearance of steeper gradients at their boundaries.

3. Energy Dissipation Rate: Assessment of Three Radar Methods

As specified in the introduction, three methods are generally proposed for estimating the energy dissipation rate from the ST radar data. The first one is based on the measurement of the return power and is referenced in the following as the "power method." Two methods make use of the spectral width measurement and are referenced in this study as "width method 1" and "width method 2" respectively. It must be specified that both power method and width method 1 require additional measurements of temperature and humidity, which may be provided by meteorological radiosondes, while width method 2 needs only radar measurements and antenna characteristics.

The power method proposed by *VanZandt* et al. [1978] and*Gage et al.* [1980] is based on the measurement of the refractive index structure constant C_n^2 (which is proportional to the backscattered power). With the hypothesis of incompressibility, isotropic and

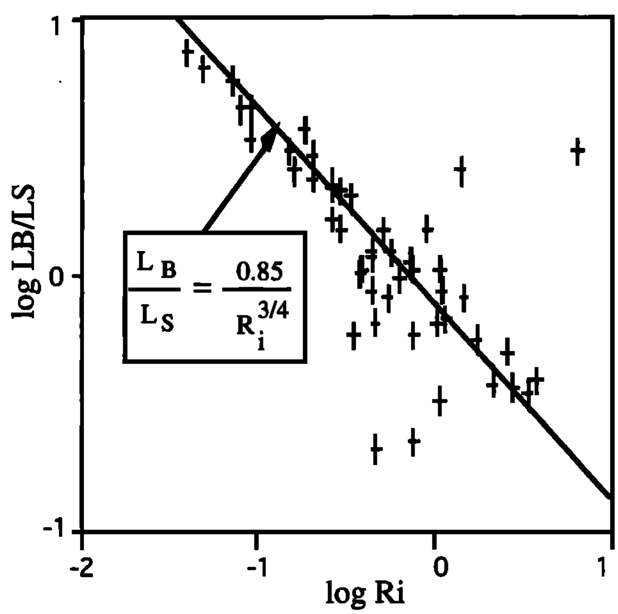

Figure 5. Evolution of the ratio L_B/L_S as a function of the gradient Richardson number R_i. The best fit (solid curve) follows the empirical law $L_B / L_S = 0.85 / R_i^{3/4}$.

stationary turbulence [after *Doviak and Zrnic* 1983], it can be shown that for high vertical resolution radars

$$\varepsilon = \left[\frac{1-R_f}{R_f} \frac{C_n^2 N^2}{a^2 M^2} \right]^{3/2} \qquad (12)$$

where a^2 is a constant, generally taken as equal to 2.8, and M is the vertical gradient of the generalized potential refractive index. This method requires a calibrated high-resolution radar as well as additional in situ measurements of temperature and humidity in order to evaluate N^2 and M^2.

As shown in the previous section, the R_f values remain in the range 0.15-0.3 in the observed turbulent layers. Moreover, it has been shown that the ST radars are generally not able to observe eroded regions within fully developed turbulent layers, but only their stratified boundaries or the initial stage of turbulent activity (turbulence setup). Under these conditions, the ratio $C_1=(1-R_f)/R_f$ might vary from $C_1=2.3$ to $C_1=5.6$. Consequently, the radar estimate of the eddy dissipation rate could be affected by an uncertainty factor of 2 or 3.

Width method 1 has been proposed by *Businger et al.* [1971], *Zeman and Tennekes* [1977], *Weinstock* [1981], and*Gossard and Strauch* [1983]. It uses the variance $\overline{w'^2}$ of the vertical turbulent wind fluctuations observed during the time interval of the corresponding observation. The use of the vertical component w' is recommended [*Weinstock*, 1981] because the vertical velocity has very little energy in wave numbers < k_B (where k_B is the buoyancy wave number), whereas the horizontal velocities may have substantial energy in wave number < k_B. The energy dissipation rate is then given by

$$\varepsilon = 0.4\overline{w'^2}N \qquad (13)$$

The wind fluctuations produce a spectral broadening of the Doppler spectrum, which is related to w'^2 by:

$$\Delta f = \frac{2}{\lambda}\left(2 \ln 2\overline{w'^2}\right)^{1/2} \qquad (14)$$

where Δf is the spectral half width induced by wind fluctuations and λ the radar wavelength. so that ε is given by

$$\varepsilon = 5\ 10^{-2} \frac{(\lambda \Delta f)^2}{\ln 2} N \qquad (15)$$

This method is much simpler in theory than the power method. However, it also requires, as for the power method, additional measurements of temperature profiles. Another difficulty in its use is the possible non turbulent contributions on the spectral width [*Spizzichino*, 1975, *Hocking*, 1996]. Only UHF radars using large antenna like Arecibo [*Ierkic et al.*, 1990], Millstone Hill [*Cohn*, 1995], or PROUST radars are well suited for this method because they have narrow antenna beams (smaller than 1°) and short pulse lengths (<1 µs).

Width method 2 has been proposed by *Frisch and Clifford* [1974],*Gossard and Strauch* [1983],*Gossard and Sengupta* [1988], and *Cohen* [1995]. For an isotropic, stationary, and homogeneous turbulence, when omitting the second-order terms, the energy dissipation rate associated with a turbulent layer observed by an ST radar may be written as

$$\varepsilon = \alpha^{-1} \frac{\overline{w'^3}}{\left[c\left(1-\frac{\gamma^2}{15}\right)\right]^{3/2}} \qquad (16)$$

with c=2.16 and $\gamma^2=4[1-(\beta/\alpha)]^2$

where α is the horizontal dimension of the volume illuminated by the antenna of beam width θ_f, at the distance r, while β is the radial dimension of the radar gate.

Equation (16) supposes that the radar is observing along the vertical and that the horizontal dimension of the illuminated volume is greater than the radar resolution ($\alpha>\beta$). This method is very interesting because it doesn't need any complementary measurements of temperature and humidity, as in the previous methods. Its limitations are the same as in width method 1; it is, however, more sensitive (due to the use of $\overline{w'^3}$ instead of $\overline{w'^2}$) to errors introduced by possible non turbulent contributions on the spectral width. Consequently, this method can only be used by UHF radars with narrow-beam antennas.

3.1. Experimental Assessment of the "Power method"

The energy dissipation rate estimated by the power method (equation (12)) can be assessed by comparing the experimental results obtained for ε within the observed turbulent layers from C_T^2 and C_V^2 measurements, respectively, the latter determination being considered as a reference. In the absence of humidity (stratospheric measurements), (12) can be rewritten as

$$\mathcal{E} = \left[\frac{1-R_f}{R_f} \frac{N^2 C_T^2}{a^2 (d\theta/dz)^2} \right]^{3/2} \tag{17}$$

Unfortunately, as stressed in section 1, the ratio $C_T^2/(d\theta/dz)$, is badly defined in regions where the potential temperature gradient is eroded by the turbulent activity, possibly giving rise to a strong dispersion in the results. Comparison of ε estimates, by using $C_V{}^2$ (equation (8)) and $C_T{}^2$ (equation (17)), respectively, in the seven turbulent layers is shown in Figure 6. The mean value R_f=0.25 has been taken in this comparison. In order to test the effect of low $d\theta/dz$ values in the dispersion of the results, regions where $d\theta/dz$ is smaller than 0.01 K/m are indicated by asterisks in Figure 6.

A reasonable agreement is found between both estimates, despite a dispersion which is partly due to the data recorded in regions of weak potential temperature gradient, and also to the variability of the ratio C_1. One can conclude that the radar estimate of ε by the power method could be affected by an uncertainty factor of 2 or 3.

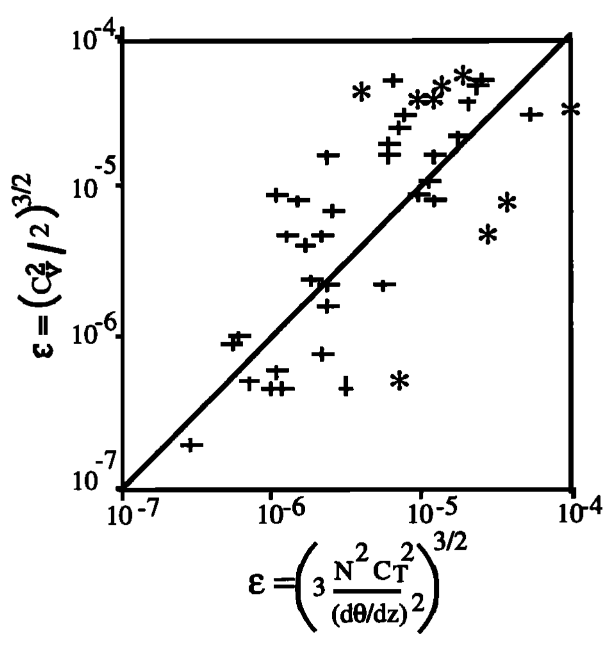

Figure 6. Assessment of the "power method." Comparison of the energy dissipation rate estimated from $C_V{}^2$ and $C_T{}^2$ in situ measurements within seven turbulent layers. Asterisks indicate regions where $d\theta/dz$ is smaller than 0.01 K/m.

3.2. Experimental Assessment of "Width Method 1"

The energy dissipation rate estimated by width method 1 (equations (13) and (15)) can also be assessed by comparing the experimental results obtained for ε within the observed turbulent layers from turbulent wind variance and structure constant $(C_V{}^2)$ measurements, respectively, the latter determination being considered as a reference.

As specified by *Weinstock* [1981], this method (equation (13)) is mainly valid when using vertical turbulent wind fluctuations. However, as stressed in section 1, the balloon-borne instruments of the experiment do not measure the vertical, only the horizontal wind fluctuations. This limitation could introduce a difficulty in the use of equation (13) if the isotropy of the atmospheric turbulence is not verified. An estimate of the deviation from isotropy has already been done by *Reiter and Burns* [1966], and *Ashburn et al.* [1968]. These authors found an average energy in the horizontal component of about twice the energy in the vertical component. This proportion is also found from the balloon experiment when comparing the horizontal outer scale L_O (experimentally provided by the structure functions of wind fluctuations) and the mixing lenth L_S (which gives the length-scale limitation by the wind shear). The mean value of the ratio L_O/L_S in the seven observed turbulent layers leads to

$$\frac{\overline{u_0^2}}{\overline{w'^2}} = \overline{\left(\frac{L_O}{L_S}\right)^{2/3}} \approx 2 \tag{18}$$

When taking (18) into account, comparison of ε estimated (in the seven turbulent layers) by (8) and (13), respectively, is given in Figure 7. When the mean potential temperature gradient is locally estimated by a running mean over an altitude range of 30-40 m, the comparison, given in Figure 7a, exhibits reasonable agreement, in spite of a rather important dispersion. This dispersion is notably reduced (Figure 7b) when the mean potential temperature gradient is estimated over the 2000-m altitude range where the seven turbulent layers are observed ($d\theta/dz$ =4x10^{-2} K m^{-1}, corresponding to the dashed line drawn in Figure 1c). This last comparison (Figure 7b) clearly shows that when $d\theta/dz$ is evaluated over a wide range of altitude, width method 1 may provide a more precise estimate of ε than the power method.

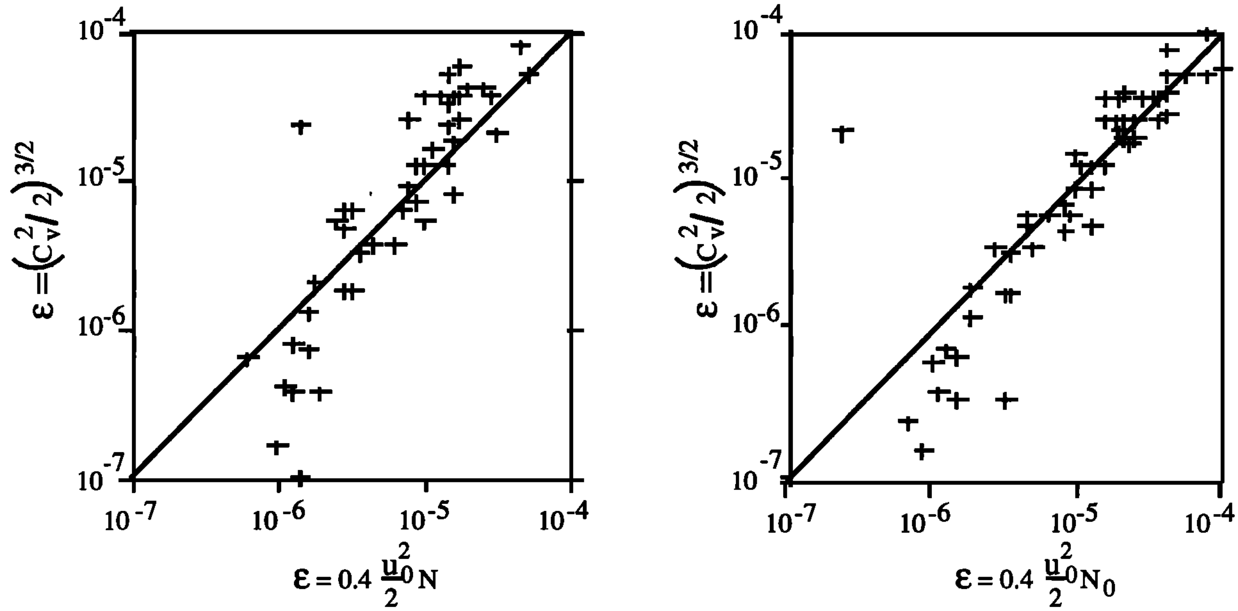

Figure 7. Assessment of "width method 1" using the seven observed turbulent layers. Comparison of the energy dissipation rate estimated from equations (8) (C_V^2) and (13) (horizontal wind variance and Brunt-Vaisala frequency). At left, the mean potential temperature gradients are estimated within each turbulent layer. At right, the mean potential temperature gradient is estimated over the 2000-m altitude range where the seven turbulent layers are observed.

3.3. Experimental Assessment of "Width Method 2"

A general assessment of equation (16) is not possible from this specific data set because it requires the knowlege of radar characteristics (beam width antenna and vertical resolution), which are clearly very different from one radar to the other. In the other hand, ST radars are generally not able to observe turbulent activity above 20 km altitude. However, one can replace equation (16) by its general form

$$\varepsilon = \frac{\overline{w'}^3}{C(z)} \tag{16'}$$

where $C(z)$ is, for a specific radar, only dependent on the altitude of the observed turbulent layer. For a given altitude, C(z) is a constant. It is then possible to calculate its value for which successive ε values derived from equation (16') (using $\overline{u_0}$ profiles measured in the seven observed turbulent layers) are more similar to ε calculated from the structure constant C_V^2 profiles. The result is given in Figure 8 and shows that the better comparison is obtained with $C(\overline{z_0}) \approx 10$. It is a

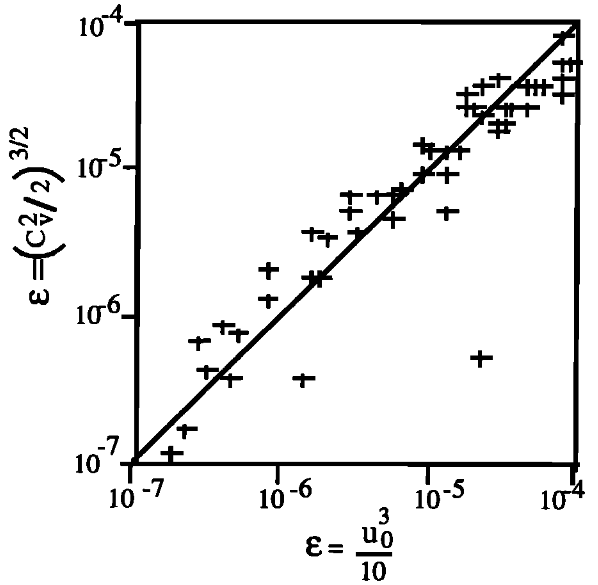

Figure 8. Assessment of "width method 2." Comparison of the energy dissipation rate estimated from equations (8) (C_V^2) and (16') (horizontal wind variance).

somewhat puzzling result. On the one hand, it clearly indicates that for a given mean altitude $\overline{z_0}$, ε is proportional to $\overline{u_0}^3$ (and then to $\overline{w'}^3$). However, on the other hand, it leads to an unrealistic value of the corresponding antenna beam width θ_f. Further investigations are apparently necessary in order to assess this method.

4. Eddy Diffusivity Generated by Small-Scale Three-Dimensional Turbulence

The eddy diffusivity can be approached in two ways: One is based on a dimensional analysis, another on using a parametrization of the turbulence. The purpose of this paper is neither to give theoretical justifications of these approaches nor to discuss the related closure problems, but only to assess different formulations of the eddy diffusivity provided in the literature by using in situ measurements of the parameters giving access to its estimate.

By analogy between molecular and eddy diffusion, the eddy diffusivity can be expressed as

$$K = u'l' \tag{19}$$

where u' is a characteristic turbulent velocity and l' is a characteristic length scale. A possible length scale is provided by the outer limit L_0 of the inertial subrange, and a good estimation of the turbulent velocity is the rms value u_o of turbulent wind fluctuations. Both parameters are given by the structure function analysis of the observed turbulent velocity fields. *Weinstock* [1978] gives a theoretical justification of the above empirical relationship and finds for K the following expression:

$$K_0 = \frac{u_o L_o}{10\sqrt{\pi}} \tag{20}$$

Another approach to the eddy diffusivity is also possible by analogy with Fourier's law for heat flux. Following this approach, the eddy diffusion coefficient for heat transfer K_θ can be considered as the heat flux per gradient unit of potential temperature:

$$K_\theta = -\overline{w'\theta'}\left(\frac{d\theta}{dz}\right)^{-1} \tag{21}$$

Similarly, it is possible to define a momentum diffusivity K_M as

$$K_M = \frac{-\overline{u'w'}}{S} \tag{22}$$

The ratio between these two diffusion coefficients is the Prandtl number P_r:

$$P_r = \frac{K_M}{K_\theta} \tag{23}$$

Taking into account the energy dissipation rate $\varepsilon = P\text{-}B$ and the flux Richardson number $R_f = B/P$, equations (21) and (22) can also be written as

$$K_\theta = \frac{R_f}{1-R_f}\frac{\varepsilon}{N^2} \tag{24}$$

or, from (12)

$$K_\theta = \left(\frac{1-R_f}{R_f}\right)^{1/2} \frac{N}{a^3 M^3}\left(C_n^2\right)^{3/2} \tag{24'}$$

and

$$K_M = \frac{1}{1-R_f}\frac{\varepsilon}{S^2} \tag{25}$$

Lilly et al. [1974], assuming R_f=0.25 in the turbulent layers, propose

$$K_\theta = \frac{\varepsilon}{3N^2} \tag{26}$$

The same assumption made for (25) leads to

$$K_M = \frac{\varepsilon}{0.75\ S^2} \tag{27}$$

Experimental results obtained with balloon-borne anemometer and thermistor measurements allows for independent estimates of K_θ and K_M by using equations (20), (26), and (27). Here u_o and L_o are obtained from structure function analysis of velocity fluctuations, ε is derived from the C_V^2 estimate, while N^2 and S^2 are obtained from filtered temperature and wind profiles. Comparisons of the eddy diffusivity profiles obtained in layer L7 are given in Figure 9.

Several remarks can be noted.

1. Only the k_θ profile provided by equation (26) dramatically differs from others estimates in regions where the potential temperature has been eroded by the

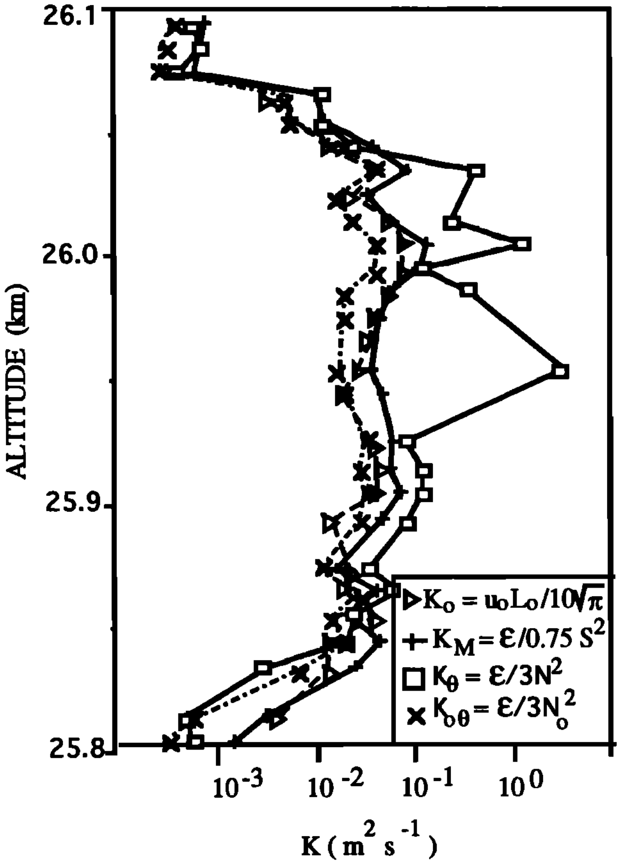

Figure 9. Vertical profiles of eddy diffusivity within turbulent layer L7 estimated by different methods. One can notice a rather good consensus between the methods, exept for the estimate using the local dθ/dz, which dramatically differs from this consensus in regions of weak dθ/dz. This discrepancy vanishes when taking into account the "nonlocal" potential temperature gradient.

turbulence, confirming that local dθ/dz and the gradient Richardson number are not the pertinent parameters for defining the eddy diffusivity. One can also verify that in these regions, the Prandtl number strongly varies.

2. By contrast, when taking into account the noneroded potential temperature profile corresponding to the dashed line drawn in Figure 1c ($d\theta/dz = 4\times10^{-2}$ K m^{-1}) and assuming that $R_f = 0.25$ within the turbulent layer, equation (24) becomes

$$K_{o\theta} = \frac{\varepsilon}{3N_0^2} \qquad (28)$$

where N_0^2 might be considered as the "initial stratification." The corresponding $K_{o\theta}$ profile is also given in Figure 9. It can be seen that this eddy diffusivity estimate is now in good agreement with K_o and K_M profiles, confirming the consistency of the above assumptions. The consequences of these results are important for the radar estimate of the eddy diffusivity by this method: Only the "nonlocal" temperature gradient (here estimated over a 2-km altitude range) must be taken into account.

3. K_o (equation 20), K_M (equation 27) and $K_{o\theta}$ (equation 28) profiles are observed to be reasonably similar within the turbulent layer, confirming the robustness of the different approaches for the eddy diffusivity estimate. In particular, the estimate corresponding to equation (20) proposed by *Weinstock* [1978] receives here a surprising validation.

4. The similarity between K_M and $K_{o\theta}$ profiles confirms the possibility of deriving the eddy diffusivity from wind shear and ε measurements. This assessment is interesting because the method requires an independent parameter S provided by ST radar measurements.

5. Conclusion

Analysis of in situ measurements of wind and temperature fluctuations in turbulent patches has provided the possibility of testing the visibility of the turbulent activity by ST radars and the capability of deriving energy dissipation rate and eddy diffusivity from radar power return and spectral width measurements, when complementary information on temperature and humidity profiles is provided (e.g. by meteorological radiosondes). The experimental data set is unfortunately limited to only a few cases of stratospheric turbulence (seven layers observed), which could limit the ability to make general statements. However, the manner in which the data have been obtained (slowly descending balloon, 30-m diameter, high-performance instrumentation, 16-Hz telemetry) allowed acquisition of a very robust data set, the main results of which are found to be in good agreement with previous works published on the boundary layer turbulence. As already observed by *Browning and Watkins* [1970], it is shown that only the initial stage of turbulence or the boundaries of the fully developed turbulent layers are generally observable by ST radars. The turbulent erosion appears to be more efficient for temperature gradients than for wind shears, so that the gradient Richardson number R_i tends toward zero within the well-developed turbulent layers while it increases toward values greater than one on their boundaries. By contrast, the flux Richardson number R_f is found to remain close to its initial critical value in the whole layer. Consequently, the Prandtl number is strongly varying within the same layer. This behavior of the Prandtl number as a function of R_i has been already noticed by *Kondo et al.* [1978] and *Gossard and Frisch* [1987] in the boundary layer. Its verification in the case of stratospheric turbulence provides an experimental basis for defining justification and limits in the use of radar methods for monitoring eddy diffusion and energy dissipation rates. Assessment of the "power method" proposed by *VanZandt et al.* [1978] and *Gage et al.* [1980], often used for estimating the energy dissipation rate ε from ST radars, has been performed by comparing results obtained from in situ measurements of C_T^2, $d\theta/dz$, and wind fluctuation variance, with ε directly derived from C_V^2 simultaneously measured. The results are reasonably similar, in spite of a rather important dispersion partly due to a bad definition of the ratio $C_T^2/(d\theta/dz)$, in eroded regions (not seen by ST radars) but also partly due to small variations of R_f in the range 0.15-0.30. This R_f variability could introduce an uncertainty factor of 2 or 3 on the energy dissipation rate estimated by ST radars when the power method is used. Assessment of two "width methods" have also been done. The first one, proposed by *Zeman and Tennekes* [1977], *Weinstock* [1981], and *Gossard and Strauch* [1983], using spectral width and Brunt-Vaisala frequency, is shown to provide a more accurate estimate of the energy dissipation rate when the potential temperature gradient is estimated over a wide altitude range (here over 2 km). Assessment of a second width method proposed by *Frisch and Clifford* [1974], *Gossard and Strauch* [1983], *Gossard and Sengupta* [1988], and *Cohen* [1995] and using both spectral width and radar characteristics (antenna beam width, radial resolution) exhibits knotty results. Further investigations and experimental comparisons between radar and balloon measurements are apparently still needed. Finally, the validity of different methods used for estimating eddy diffusion coefficients has been tested by comparing the deduced profiles in a given turbulent layer from in situ measurements of C_V^2, $d\theta/dz$, wind fluctuations variance, outer scale of turbulence, and wind shear. The profiles obtained are quite similar, whatever the method used. This comparison clearly indicates that the well-known relationship $K_\theta=(R_f/1-R_f)(\varepsilon/N^2)$ is valid (but affected by relatively large error bars) when taking (1) R_f=0.25 and (2) N deduced from the "non-local" potential temperature gradient (i.e. over an altitude range much wider than the turbulent layer thickness).

Acknowledgments. This experimental study was supported by the Centre National d'Etudes Spatiales and by the Institut National des Sciences de l'Univers.

References

Ashburn, E. V., D. T. Prophet, and D. E. Waco, High altitude clear air turbulence models of aircraft design and operation, *Tech. Rep. AFFDL-TR-68-79*, Air Force Flight Dyn. Lab., Wright-Patterson Air Force Base, Ohio, 1968.

Barat, J., Some characteristics of clear air turbulence in the middle stratosphere, *J. Atmos. Sci., 39,* 2553-2564, 1982.

Barat, J., and F. Bertin, On the contamination of stratospheric turbulence measurements by wind shear, *J. Atmos. Sci., 41*, 819-827, 1984a.

Barat, J., and F. Bertin, Simultaneous measurements of temperature and wind velocity fluctuations within C.A.T.: Analysis of the estimate of dissipation rate by remote sensing techniques, *J. Atmos. Sci., 41*(9), 1613-1619, 1984b.

Businger, J.A., J.C. Wyngaard, Y. Izumi, and E.F. Bradley, Flux-profile relationships in the atmospheric surface layer, *J Atmos. Sci., 28*, 181-189, 1971.

Browning, K. A., and C. D. Watkins, Observation of clear air turbulence by high power radar, *Nature, 227*, 260-263, 1970.

Cohn, S. A., Radar measurements of turbulent eddy dissipation rate in the tropopshere: A comparison of techniques, *J. Atmos. Oceanic Technol., 12*, 85-95, 1995.

Crane, R., K., A review of radar observations of turbulence in the lower stratosphere, *Radio Sci., 15*(2), 177-193, 1980.

Dalaudier, F., C. Sidi, M. Crochet, and J. Vernin, Direct evidence of "sheets" in the atmospheric temperature field, *J. Atmos. Sci., 51*(2), 237-248, 1994.

Delage, D., R. Roca, F. Bertin, J. Delcourt, A. Crémieu, M. Massebeuf, R. Ney, and P. Van Velthoven, A consistency check of three radar methods for monitoring eddy diffusion and energy dissipation rates through the tropopause, *Radio Sci.* 96RS-03543, this issue.

Dillon, T. M., Vertical overturning: A comparison of Thorpe and Ozmidov length scales, *J. Geophys. Res., 87*(C12), 9601-9613, 1982.

Dougherty, J. P., The anisotropy of turbulence at meteor level, *J. Atmos. Terr. Phys., 21*, 210-213, 1961.

Doviak, R.J. and D.S. Zrnic, Reflection and scatter formula for anisotropically turbulent air, *Radio Sci., 19*(1), 325-336, 1984.

Frisch, A. S., and S. F. Clifford, A study of convection capped by a stable layer using Doppler radar and

acoustic echo sounders, *J. Atmos. Sci., 31*, 1622-1628, 1974.
Gage, K. S., J. L. Green, and T. E. VanZandt: Use of Doppler radar for the measurement of atmospheric turbulence parameters from intensity of clear-air echoes, *Radio Sci., 15*(2), 407-416, 1980.
Gossard, E.E., and A. S. Frisch, Relationship of the variances of temperature and velocity to atmospheric static stability - Application to radar and acoustic sounding, *J. Clim. Appl. Meteorol., 26*, 1021-1036, 1987.
Gossard, E. E., and N. Sengupta, Measuring gradients of meteorological properties in elevated layers with a surface-based Doppler radar, *Radio Sci., 23*(4), 625-639, 1988.
Gossard, E. E., and R. G. Strauch, *Radar Observations of Clear Air and Clouds*, 280 pp., Elsevier, New York, 1983.
Hocking, W. K., Measurement of turbulent energy dissipation rates in the middle atmosphere by radar techniques: A review, *Radio Sci., 20*(6), 1403-1422, 1985.
Hocking, W. K., An assessment of the capabilities and limitations of radar in measurements of the upper atmosphere turbulence, *Adv. Space Res., 17*(11), 1137-1147, 1996.
Ierkic, H.M., R.F. Woodman, and P. Perillat, Ultrahigh vertical resolution radar measurements in the lower stratosphere at Arecibo, *Radio Sci., 25*(5), 941-952, 1990.
Kondo, J., O. Kanechika, and N. Yasuda, Heat and momentum transfers under strong stability in the atmospheric surface layer, *J. Atmos. Sci., 35*, 1012-1021, 1978.
Lilly, D. K., D.E. Waco, and S.I. Adelfang, Stratospheric mixing estimates from high-altitude turbulence measurements, *J. Appl. Meteorol., 13*, 488-493, 1974.
Lübken, F.-J. On the extraction of turbulent parameters from atmospheric density fluctuations, *J. Geophys. Res., 97*(20), 20,385-20,395, 1992.
Lübken, F.-J., U. Von Zahn, E.V. Thrane, T. Blix, G.A. Kokin, and S. V. Pachomov, In situ measurements of turbulent energy dissipation rates and eddy diffusion coefficients during MAP/WINE, *J. Atmos. Terr. Phys., 49*, 763-775, 1987.
McIntyre, M. E., On dynamics and transport near the polar mesopause in summer, *J. Geophys. Res., 94*(D12), 14,617-14,628, 1989.
Moum, J. N., The quest for K_ρ - Preliminary results from direct measurements of turbulent fluxes in the ocean, *J. Phys. Oceanogr., 20*, 1980-1984, 1990.
Ottersten, H., Atmospheric structure and radar backscattering in clear air, *Radio Sci., 4*(12) 1179-1193, 1969.
Reiter, E. R., and A. Burns The structure of clear-air turbulence derived from "TOPCAT" aircraft measurements, *J. Atmos. Sci., 23*, 206-212, 1966.
Sengupta, N., J. N. Warnock, E. E. Gossard, and R. G. Strauch, Remote sensing of meteorological paramaters with the aid of a clear-air Doppler radar, *NOAA Tech. Rep., ERL-431-WPL 61*, 27 pp., 1987.
Spizzichino, A., Spectral broadening of acoustic and radio waves scattered by atmospheric turbulence in the case of radar and sodar experiments, *Ann. Geophys., 31*(4), 433-445, 1975.
Tatarskii, V. I.: *Wave propagation in a turbulent medium*, Translated by R. A. Silverman, 285 pp., McGraw-Hill, New York, 1961.
Thorpe, S.A., Experiments on the instability of stratified shear flows: Mixable fluids, *J. Fluid Mech., 46*, 299-319, 1971.
Thorpe, S. A., Turbulence in stably stratified fluids: a review of laboratory experiments, *Boundary Layer Meteorol., 5*(1-2), 95-119, 1973.
Thrane, E. V.,and B. Grandal, Observation of fine-scale structure in the mesosphere and lower thermosphere, *J. Atmos. Terr. Phys., 43*, 179-189, 1981.
Thrane, E. V., T. A. Blix, C. Hall, T. L. Hansen, U. vonZahn, W. Meyer, P. Czechowsky, G. Schmidt, H. U. Winddel, and A. Neuman, Small-scale structure and turbulence in the mesosphere and lower thermosphere at high latitudes in winter, *J. Atmos. Terr. Phys., 49*, 751-762, 1987.
VanZandt, T. E., J. L. Green, K. S. Gage, and W. L. Clark, Vertical profiles of refractivity turbulence structure constant: Comparison of observations by the Sunset radar with a new theoretical model, *Radio Sci., 13*(5), 819-829, 1978.
Vinnichenko, N. K., N. Z. Pinus, S. M. Shmeter, and G. N. Shur, *Turbulence in the Free Atmosphere*, 263 pp., Consult. Bur., New York, 1973.
Weinstock, J., Vertical turbulent diffusion in a stable stratified fluid, *J. Atmos. Sci., 35*, 1022-1027, 1978.
Weinstock, J., Energy dissipation rates of turbulence in the stable free atmosphere, *J. Atmos. Sci, 38*, 880-883, 1981.
Woodman R.F., and P.K. Rastogi, Evaluation of effective eddy diffusive coefficients using radar observations of turbulence in the stratosphere, *Geophys. Res. Lett., 11*(3), 243-246, 1984
Zeman, O., and H. Tennekes, Parametrization of the turbulent energy budget at the top of the daytime atmospheric boundary layer, *J. Atmos. Sci., 34*, 111-123, 1977.

J. Barat and R. Wilson, Service d'Aéronomie du CNRS, BP 3, 91371 Verrières le Buisson, France. (e-mail: jean.barat@aerov.jussieu.fr; charles.cot@aerov.jussieu.fr)
F. Bertin, Centre d'Etude des Environnements Terrestres et Planétaires, 4, Av. de Neptune, 94107 Saint Maur-des-Fossés, France. (e-mail: francois.bertin@cetp.ipsl.fr)

(Received June 18, 1996; revised October 25, 1996; accepted November 19, 1996.)